Recombinant ADAMTS-1 promotes muscle regeneration accompanied by downregulation of Notch signaling

JIN-HWA KIM[1], SANG-HYUP LEE[2], SANG-YOON KIM[2], JEONG-WON KIM[1,3], JI-SOO JEONG[1], EUN-HYE CHUNG[1], SU-HA LEE[1], CHANG-YEOP KIM[1], BONG-KEUN CHOI[2], JE-WON KO[1] and TAE-WON KIM[1]

[1]Department of Veterinary Medicine, College of Veterinary Medicine (BK21 FOUR Program), Chungnam National University, Daejeon 34131, Republic of Korea; [2]Nuon Bio Co., Ltd., Seongnam, Gyeonggi 13201, Republic of Korea; [3]Laboratory of Radiation Exposure and Therapeutics, National Radiation Emergency Medical Center, Korea Institute of Radiological and Medical Sciences, Seoul 01812, Republic of Korea

Received July 30, 2025; Accepted November 27, 2025

DOI: 10.3892/ijmm.2025.5718

Abstract. Skeletal muscle satellite cells (MuSCs) play a central role in muscle regeneration; however, their capacity declines with age, contributing to sarcopenia. A disintegrin and metalloproteinase with thrombospondin motifs-1 (ADAMTS-1) regulates MuSC activation and differentiation. The present study aimed to investigate the potential of recombinant ADAMTS-1 (rADAMTS-1) as a therapeutic strategy to enhance MuSC proliferation and improve regeneration. After barium chloride injection, mice received daily intraperitoneal injections of rADAMTS-1 at 5 or 10 mg/kg for 1, 3, 7, or 14 days to monitor recovery. Primary skeletal muscle and C2C12 cells were also treated with rADAMTS-1 to evaluate its effects on gene and protein expression during proliferation and differentiation *in vitro*. The number of MuSCs and the expression of myogenic markers increased in all injured groups by day 3 post-injury *in vivo*. These levels were particularly elevated in the high-dose rADAMTS-1 group and remained sustained until day 14. Grip strength recovered to normal levels by day 7 in the high-dose rADAMTS-1 group, suggesting improved functional recovery compared with the untreated controls. *In vitro*, rADAMTS-1 treatment induced a dose-dependent increase in muscle fiber length and upregulation of regeneration-related factors in primary skeletal muscle cells. Furthermore, C2C12 cells treated with rADAMTS-1 exhibited enhanced expression of myocyte developmental genes during differentiation. The findings highlighted the therapeutic potential of rADAMTS-1 for sarcopenia, potentially addressing limitations associated with conventional MuSC-based treatments.

Correspondence to: Professor Je-Won Ko or Professor Tae-Won Kim, Department of Veterinary Medicine, College of Veterinary Medicine (BK21 FOUR Program), Chungnam National University, 99 Daehak-ro, Daejeon 34131, Republic of Korea
E-mail: rheoda@cnu.ac.kr
E-mail: taewonkim@cnu.ac.kr

Abbreviations: ADAMTS-1, a disintegrin and metalloproteinase with thrombospondin motifs 1; $BaCl_2$, barium chloride; Con, control; CD, cluster of differentiation; dpi, days post-injection; eMyHC, embryonic myosin heavy chain; GO, Gene Ontology; Hes-1, hairy and enhancer of split-1; MuSC, skeletal muscle satellite cells; Myf6, myogenic factor 6; Myh1, myosin heavy chain 1; Myh 2, myosin heavy chain 2; Myh4, myosin heavy chain 4; Mymx, myomixer; MyoD, myoblast determination protein 1; MyoG, myogenin; NC, non-injured control; NICD, Notch intracellular domain; Pax7, paired box protein 7; rADAMTS-1, recombinant ADAMTS-1; rADAMTS-1 (L), rADAMTS-1 at 5 mg/kg; rADAMTS-1 (H), rADAMTS-1 at 10 mg/kg; Sca1, stem cell antigen 1; TA, tibialis anterior; VCAM1, vascular cell adhesion molecule

Key words: ADAMTS-1, notch intracellular domain, recombinant ADAMTS-1, sarcopenia, skeletal muscle regeneration, skeletal muscle satellite cell

Introduction

Sarcopenia is a progressive and multifactorial condition characterized by the loss of skeletal muscle mass, strength, and function and is frequently observed in older adults (1). This age-associated decline contributes to frailty, functional deterioration, and increased healthcare costs (2,3). Despite the clinical burden, no approved pharmacological treatments are available to effectively enhance muscle regeneration in patients with sarcopenia (4,5). Developing novel strategies to improve muscle repair remains a significant challenge.

Impaired function of skeletal muscle satellite cells (MuSCs), which are indispensable for post-injury muscle regeneration, is recognized as a central mechanism underlying sarcopenia. In response to muscle damage, MuSCs become activated, proliferate, and differentiate along the myogenic lineage to support effective repair of damaged fibers (6,7). Aging leads to a decline in both the number and functional capacity of MuSCs, resulting in impaired regenerative ability and exacerbated muscle wasting (8). Although direct cell transplantation has been proposed as a potential approach,

clinical application is limited by technical and immunological barriers, such as challenges in determining the optimal timing, delivery route, and transplantation site (9,10). Therefore, stem cell-mediated therapy has gained attention as a potential strategy to support muscle regeneration in aging muscles, particularly to overcome the practical challenges associated with transplantation-based therapies (5).

Among various candidates, a disintegrin and metalloproteinase with thrombospondin motifs 1 (ADAMTS-1) has been identified as a regulator of early myogenesis (11). Its expression increases during MuSC proliferation and promotes myogenic differentiation, partly by reducing the Notch intracellular domain (NICD), which modulates the Notch signaling pathway (12). Given the importance of Notch signaling in balancing MuSC quiescence and activation, targeting this axis via ADAMTS-1 may offer therapeutic benefits for enhancing muscle regeneration in aging populations (13).

The present study investigated whether recombinant ADAMTS-1 (rADAMTS-1), comprising a condensed pro-domain and metalloproteinase domain, enhances MuSC-mediated regeneration by modulating myogenic signaling. The effects of rADAMTS-1 on MuSC proliferation, differentiation, and functional recovery were evaluated using *in vivo* and *in vitro* models. A barium chloride ($BaCl_2$)-induced acute skeletal muscle injury model was employed to induce localized myofiber necrosis while sparing MuSCs, thereby enabling reproducible assessment of muscle regeneration (14). Although this model does not mimic the chronic features of sarcopenia, it provides a robust platform for studying rapid muscle damage and subsequent MuSC self-renewal and myoblast expansion (15). Findings from this model may contribute to the development of strategies to address delayed muscle regeneration in the elderly, where impaired MuSC function and altered regeneration timing hinder effective recovery (8).

The present study evaluated whether rADAMTS-1 promoted MuSC proliferation and differentiation, highlighting its role in muscle regeneration and the Notch signaling pathway. This approach may help overcome limitations associated with MuSC transplantation and support the advancement of targeted therapies for sarcopenia.

Materials and methods

Production and purification of rADAMTS-1. The cloning and mutagenesis of ADAMTS-1 were performed following protocols previously described by Lee *et al* (13). Full-length ADAMTS-1 cDNA was generated by reverse transcription (RT)-PCR using a human cDNA library and subcloned into a mammalian expression pEF/V5-polyhistidine (His) vector (Invitrogen; Thermo Fisher Scientific, Inc.). Various randomly deleted ADAMTS-1 mutants were generated using In-Fusion® cloning tools (Takara Bio, Inc.). The ADAMTS-1 expression plasmid used in the present study was prepared in-house and a 1 mg/ml stock was generated for transfection.

Chinese hamster ovary (CHO)-K1 cells (CCL-61; ATCC) were used for the production of rADAMTS-1. rADAMTS-1 overexpressed CHO cells were cultured in an ExpiCHO expression medium (cat. no. A2910002; Gibco; Thermo Fisher Scientific, Inc.) at 37˚C in a humidified 5% CO_2 incubator. Cells were transfected with 4 μg plasmid DNA per 100 mm dish using Lipofectamine® 2000 (Invitrogen; Thermo Fisher Scientific, Inc.). After 24 h of incubation at 37˚C, and single cell-derived clones were selected using 5 μg/ml blasticidin (cat. no. SBR00022; MilliporeSigma) for ~2 weeks to establish stable clonal CHO cells. A stable CHO-K1 line transfected with the pEF/V5-His empty vector was generated in parallel and used as the negative control.

rADAMTS-1 was purified from cell culture supernatants of stable clones using a nickel nitrilotriacetic acid agarose column (cat. no. 31314; Qiagen GmbH). Proteins were bound for 1 h at 16˚C with gentle agitation, followed by washing and elution. The eluted rADAMTS-1 proteins were dialyzed at 4˚C overnight in phosphate-buffered saline (PBS) and used for intraperitoneal (IP) injection in mice or *in vitro* experiments. Overexpression of rADAMTS-1 was confirmed by western blot analysis (Fig. S1).

Animal study. A total of 96 mice were used in the present study and weighed 20-22 g at the start of the experiment. Specific-pathogen-free male C57BL/6 mice (7 weeks old) were obtained from Samtako Bio Korea Co., Ltd. The mice were housed under standard laboratory conditions (22±2˚C with 55±5% humidity and a 12-h light/dark cycle) with *ad libitum* access to tap water and standard rodent chow (Samyang Foods Co., Ltd.). All experimental procedures received approval from Chungnam National University Animal Care and Use Committee (approval no. 202310A-CNU-169).

After 1-week acclimation period, the mice were divided into four groups based on time points post-injection: 1, 3, 7 and 14 days (dpi). Each time point included four subgroups (n=6 per group): i) the non-injured control (NC), ii) $BaCl_2$ (cat. no. 202738; MilliporeSigma): $BaCl_2$ intramuscular (IM) injection, iii) low-dose rADAMTS-1 [rADAMTS-1 (L)]: $BaCl_2$ IM + 5 mg/kg rADAMTS-1 IP injection and iv) high-dose rADAMTS-1 [rADAMTS-1 (H)]: $BaCl_2$ IM + 10 mg/kg rADAMTS-1 IP injection. A single injection of 1.2% (w/v) $BaCl_2$ solution in saline was injected into the tibialis anterior (TA) of each mouse (except the NC group) under 2% isoflurane anesthesia. Anesthesia was induced over 5-7 min and maintained throughout the procedure to minimize pain and distress. Daily IP administration of rADAMTS-1 at low and high concentrations was continued until autopsy.

In addition, to examine whether rADAMTS-1 alone affects myogenic marker expression under non-injury conditions, a separate validation experiment was conducted. Mice received IP injection of rADAMTS-1 (10 mg/kg) without $BaCl_2$-induced injury, and TA muscles were analyzed using western blotting.

The dose of 5 and 10 mg/kg rADAMTS-1 were selected based on pilot experiments, in which a higher dose (20 mg/kg) did not produce a substantial difference compared with 10 mg/kg (Fig. S2). Therefore, 5 and 10 mg/kg were chosen as effective and practical doses for subsequent analyses. IP administration was employed because it ensures minimizing stress and potential injury to rodent (16). In addition, IP injection allows rapid and efficient absorption while avoiding degradation or modification in the gastrointestinal tract (17).

Autopsies were performed at 1, 3, 7, and 14 dpi to evaluate the temporal progression of muscle recovery after injury.

Mice were euthanized by 5% of isoflurane inhalation prior to mortality and loss of respiration and reflexes was confirmed before tissue collection. For pharmacokinetic profiling, blood samples were collected at 0 (immediately after dosing), 0.5, 1, 2, 4, 8, 24, and 48 h after a single IP injection of rADAMTS-1 (10 mg/kg) and plasma rADAMTS-1 concentrations were quantified using an immunoassay according to the manufacturer's protocol.

Grip strength. The grip strength test is widely used to assess skeletal muscle function (18). A computerized grip-strength meter (cat. no. 47200; Ugo Basile SRL) was used to measure grip strength in mice. To prevent interference during the assessment, the mice were gently held at the base of the tail and allowed to grasp a wooden stick with their forepaws. The hind paws then grasped the transducer metal bar of the apparatus, while the conductor pulled the mice backward by the tails until the grip was released. The device recorded the peak force exerted during this procedure in grams (g). All measurements were performed in a blinded manner. Each mouse underwent a minimum of 10 trials, and the median force value was recorded. Grip strength values were normalized to body weight to account for weight fluctuations throughout the experimental period.

Histopathological analysis of skeletal muscle tissue. TA tissue samples were preserved in 10% (v/v) neutral-buffered formalin, and fixation was performed at 20-23˚C. After 1 week of fixation, the tissues were dehydrated using an automated tissue processor (TP1020; Leica Biosystems), which sequentially transferred the samples through graded ethanol (70, 80, 95, and 100%) and xylene solutions, with each step lasting 1 h. The processed tissues were then paraffin-embedded, with the transverse plane positioned downward, and sectioned into 4-μm-thick slices using HistoCore BIOCUT (cat. no. 149BIO000C1; Leica Biosystems). Following a standard rehydration procedure, the slides were stained with hematoxylin and eosin (cat. nos. H08-500R and EY07-500R; TissuePro Technology). The slides were then mounted using VectaMount® Express mounting medium (cat. no. H5700; VectorLabs).

MuSC counts in TA. The harvested TA muscles were minced and digested in 0.2% collagenase type II (cat. no. 17101015; Gibco; Thermo Fisher Scientific, Inc.) in Dulbecco's Modified Eagle's medium (DMEM; cat. no. SH30243.01; Cytiva) for 90 min at 37˚C, following a modified isolation protocol previously reported (19). The digested suspensions were centrifuged at 250 x g for 10 min at 4˚C, and then passed through 70- and 40-μm cell strainers (cat. no. 93070, 93040; SPL Life Sciences). Cell counting was performed using a hemocytometer, and the suspensions were diluted to $1x10^6$ cells/ml in staining buffer (cat. no. 554657; BD Pharmingen) for analysis. All the cells were stained with antibodies recognizing MuSC markers, including cluster of differentiation (CD) 45 (1:100; cat. no. 557235; BD Biosciences), CD 31 (1:100; cat. no. 558738; BD Biosciences), and vascular cell adhesion molecule-1 (VCAM-1; 1:100; cat. no. orb623587; Biorbyt, Ltd.), and stem cell antigen 1 (Sca1; 1:100; cat. no. 108122; BioLegend, Inc.). Staining was conducted on ice for 30 min in the dark. After washing, flow cytometry data were collected using the BD Accrui C6 Plus flow cytometer (BD Biosciences).

Immunofluorescence. Histological sections underwent antigen retrieval in citrate buffer (pH 6.0; cat. no. 21545; MilliporeSigma) for 15 min at 95˚C. Subsequently, sections were blocked/permeabilized with PBS containing 0.1% Triton X-100 and 1% bovine serum albumin (cat. no. A3311; MilliporeSigma) for 30 min at 25˚C. Slides were stained with primary antibodies and diluted in blocking buffer at 4˚C overnight. MuSCs were visualized by staining for paired box protein 7 (Pax7; 1:100; cat. no. ab187339; Abcam), and regenerating myofibers were identified through MyoD staining (1:100; cat. no. GTX636812; GeneTex, Inc.). After staining, all samples were washed with PBS containing 0.1% Tween 20 (0.1% PBST) and incubated at 25˚C for 1 h with Goat Anti-Rabbit IgG H&L (Alexa Fluor® 488; 1:500; cat. no. ab150081; Abcam). Nuclei were visualized using DAPI mounting medium (cat. no. ab104139; Abcam). The samples were viewed using a fluorescence microscope (Leica Microsystems GmbH), and quantitative image analysis was performed using ImageJ software (NIH; 1.49v).

Primary skeletal muscle cells were seeded at a density of $5x10^4$ cells/well in a 24-well plate containing 1 ml of complete expansion medium. After the cells reached >90% confluence, rADAMTS-1 protein was added to the skeletal muscle differentiation medium at concentrations of 0.001, 0.01, 0.1, 1, and 10 ng/ml. After 72 h of differentiation, the cells were fixed, washed, and treated with anti-myosin heavy chain antibodies (1:100; cat. no. 05-716; MilliporeSigma). Differentiated myotubes were visualized with goat anti-mouse IgG Alexa Fluor 555 antibodies (1:500; cat. no. A-21422; Invitrogen; Thermo Fisher Scientific, Inc.) via fluorescence microscopy. Fluorescence images were obtained using a microscope (Nikon Eclipse Ts2-FL; Nikon Corporation). Myotube length was measured and calculated as the average of five samples using NIS-Elements imaging software (Nikon Corporation; 5.00v).

Immunohistochemistry. Embryonic myosin heavy chain (eMyHC) expression in TA tissues was evaluated using VECTASTAIN® Elite® ABC-HRP Kits (cat. no. PK-6101 and PK-6102; Vector Laboratories, Inc.) following the manufacturer's instructions. The paraffin sections were deparaffinized, rehydrated, and subjected to antigen retrieval for 5 min at 121˚C in citric acid buffer (pH 6.0). The slides were subsequently blocked with 10% goat serum supplied within the kit (Vector Laboratories, Inc.) for 30 min at 20-23˚C and incubated with the primary antibody (eMyHC; 1:100; cat. no. F1.652; Developmental Studies Hybridoma Bank) overnight at 4˚C. The biotinylated secondary antibody working solution was prepared according to the manufacturer's drop-based protocol and applied for 30 min at 20-23˚C. The ABC reagent was prepared using the manufacturer's recommended drop-based protocol and incubated with the avidin-biotin-peroxidase complex for 30 min at 20-23˚C. Protein expression was analyzed using a 3,3'-diaminobenzidine substrate kit (cat. no. ab64238; Abcam). The sections were counterstained with hematoxylin for 30 sec at 20-23˚C and images were captured using a light microscope, with scale bars indicated

in the figure legends. The quantitative analysis was performed using ImageJ software (NIH; 1.49v).

Western blotting. The harvested TA tissues were homogenized at a 1:10 (w/v) ratio in tissue lysis/extraction reagent (cat. no. C3228; MilliporeSigma) supplemented with protease and phosphatase inhibitors (cat. nos. 04693116001, 4906837001; Roche Diagnostics). Homogenization was performed using a BIOPREP-24R (Hangzhou Allsheng Instruments Co., Ltd.). Protein concentrations were determined using bicinchoninic acid reagents (cat. nos. 23228 and 1859078; Thermo Fisher Scientific, Inc.). Equal amounts of total protein (20 μg) were separated by 6, 10 and 15% sodium dodecyl sulfate-polyacrylamide gel electrophoresis and transferred onto polyvinylidene fluoride membranes (cat. no. IPVH00010; MilliporeSigma). The membranes were blocked for 1 h at 20-23˚C in 5% bovine serum albumin (cat. no. A9418; Sigma-Aldrich; Merck KGaA) in 0.1% PBST, and then incubated overnight at 4˚C with primary antibodies: myoblast determination protein 1 (MyoD) (1:1,000; cat. no. ab64159; Abcam), myogenin (MyoG) (1:1,000; cat. no. ab124800; Abcam), ADAMTS-1 (1:1,000; cat. no. ab276133; Abcam), NICD (1:500; cat. no. ab52301; Abcam), and Hes-1 (1:1,000; cat. no. ab71559; Abcam). After two washes with 0.1% PBST, the membranes were incubated at 25˚C for 2 h with a 1:5,000 dilution of horseradish peroxidase-conjugated secondary antibody (rabbit: cat. no. LF-SA8001; mouse: cat. no. LF-SA8002; Abfrontier Co., Ltd.). Next, the blots were washed twice with 0.1% PBST and developed using an enhanced chemiluminescence kit (cat. no. BWF0100; Biomax Co., Ltd.). Protein bands were visualized using a ChemiDoc device (io-Rad Laboratories, Inc.) and quantified using ImageJ software (NIH; 1.49v). Total protein loading was assessed by Ponceau S staining (Fig. S3), which served as the normalization standard instead of housekeeping proteins such as β-actin, GAPDH, or α-tubulin, whose expression varies in skeletal muscle (20,21). Following previous reports (22,23), the intensity of each target band was normalized to the total lane density, calculated as the sum of all visible bands within the same lane, and expressed as relative intensity.

Primary skeletal muscle cells were treated with rADAMTS-1 protein at a concentration of 10 ng/ml at the onset of differentiation using skeletal muscle differentiation tool medium. After 3 days of differentiation, the cells were harvested for western blot analysis. Primary skeletal muscle cells were lysed in CelLytic M buffer (cat. no. C2978; MilliporeSigma) and all subsequent steps followed the same procedures as described for the *in vivo* western blot protocol.

Cell culture and differentiation. Primary skeletal muscle cells (cat. no. PCS-950-010; ATCC) were cultured in a complete expansion medium (cat. no. PCS-500-030; ATCC) using a primary skeletal muscle cell growth kit (cat. no. PCS-950-040; ATCC). For differentiation, the cells were treated with a skeletal muscle differentiation tool (cat. no. PCS-950-050; ATCC) upon reaching 90% confluence. Mouse myoblast C2C12 cells (cat. no. CRL-1772; ATCC) were obtained from ATCC. C2C12 cells were cultured in DMEM (Gibco; Thermo Fisher Scientific, Inc.) supplemented with 10% fetal bovine serum (cat. no. 35-015-CV; Corning Life Sciences). C2C12 cells were incubated in DMEM containing 2% horse serum until they reached 90% confluence. Cells were used within 10 passages from thawing to ensure phenotypic consistency.

Bromodeoxyuridine (BrdU) assay. Primary skeletal muscle cells were seeded in 96-well plates at a density of $1x10^4$ cells/well and incubated with 10X BrdU solution from the BrdU assay kit (cat. no. 6813; Cell Signaling Technology, Inc.) at concentrations of 0.001, 0.01, 0.1, 1, or 10 ng/ml rADAMTS-1 for 24 h. The cells were fixed and treated with a detection antibody solution at 24˚C for 1 h. After removing the solution and washing the plate three times, the cells were incubated with a horseradish peroxidase-conjugated secondary antibody for 30 min at 24˚C. The cells were then incubated at 24˚C for 30 min with 3,3',5,5'-tetramethylbenzidine substrate, and absorbance was measured at 450 nm.

RNA-seq analysis. C2C12 cells were treated with 10 ng/ml rADAMTS-1 and differentiated for 3 days. Total RNA was isolated using the Quant-it RiboGreen RNA assay kit (cat. no. R11490; Invitrogen; Thermo Fisher Scientific, Inc.) according to the manufacturer's protocol. The total RNA integrity of the samples was assessed using the TapeStation RNA ScreenTape (cat. no. 5067-5576; Agilent Technologies, Inc.). Only high-quality RNA samples (RNA integrity number >7.0) were used for RNA library preparation. cDNA was prepared using SuperScript II Reverse Transcriptase (cat. no. 18064014; Invitrogen; Thermo Fisher Scientific, Inc.) and random primers. The products were purified and enriched using PCR to construct a final cDNA library. Library concentration was measured using KAPA Library Quantification kits for Illumina sequencing platforms, following the qPCR Quantification Protocol Guide (Kapa Biosystems, Inc.), and their quality was assessed using TapeStation ScreenTape (Agilent Technologies, Inc.). Indexed libraries were submitted for paired-end (2x100 bp) sequencing on the Illumina NovaSeq platform (Illumina Inc.), which was conducted by Macrogen Inc.

Reverse transcription-quantitative (RT-q) PCR. For RT-qPCR validation, total RNA was extracted using the easy-BLUE Total RNA Extraction Kit (cat. no. 17061; iNtRON Biotechnology DR), and 1 μg RNA was reverse transcribed using the HiSense cDNA Synthesis Master Mix (cat. no. CDS-400, CellSafe Co., Ltd.) following the manufacturer's instructions. The qPCR was performed using the QuantStudio 3 Real-Time PCR System (cat. no. A28567; Applied Biosystems; Thermo Fisher Scientific, Inc.) and SYBR Green PCR Master Mix (cat. no. 4344463; Applied Biosystems; Thermo Fisher Scientific, Inc.). The thermocycling protocol was: Initial denaturation at 95˚C for 10 min, followed by 40 cycles of 95˚C for 15 sec, 60˚C for 15 sec, and 72˚C for 45 sec. A melting curve analysis was performed from 60˚C to 95˚C to verify amplification specificity. Gene expression levels were calculated using the $2^{\Delta\Delta Cq}$ method (24) and all reactions were performed in triplicates. The following primers were used (5'-3'): Myomixer (*Mymx*), forward (F): GACCACTCCCAGAGGAAGGA, reverse (R): GGACCGACGCCTGGACTAAC; myogenic factor 6 (*Myf6*), F: TGCTAAGGAAGGAGGAGCAA, R: CCTGCTGGGTGA

AGAATGTT; myosin heavy chain 1 (*Myh1*), F: CGGAGG AACAATCCAATGTC, R: TGGTCACTTTCCTGCACTTG; myosin heavy chain 2 (*Myh2*), F: TCTCAGGCTTCAGGA TTTGG, R: CAGCTTGTTGACCTGGGACT; myosin heavy chain 4 (*Myh4*), F: CGTCAAGGGTCTTCGTAAGC, R: ATT GTTCCTCAGCCTCCTCA; and glyceraldehyde-3-phosphate dehydrogenase (GAPDH), F: CCAATGTGTCCGTCGTGG ATCT, R: GTTGAAGTCGCAGGAGACAACC. All primers were synthesized by Bioneer.

Statistical analysis. Quantitative data were presented as mean ± standard deviation. Data normality was assessed using the Shapiro-Wilk test. For normally distributed data, one-way analysis of variance with Tukey's post hoc test was used to evaluate differences among groups. The data were analyzed and the statistical graphs were constructed using GraphPad Prism 8.0 (Dotmatics). Statistical significance was defined as *P<0.05, **P<0.01, and ***P<0.001. P<0.05 was considered to indicate a statistically significant difference.

Results

Effects of rADAMTS-1 on functional and histological recovery in injured skeletal muscle. Prior to assessing its regenerative effects, systemic exposure of rADAMTS-1 following IP administration was confirmed (Fig. S4). Grip strength analysis revealed rapid recovery of grip force in the high-dose treatment group (Fig. 1A). At 1 dpi, grip force relative to body weight decreased by ~25% in the $BaCl_2$ group compared with the NC group (P<0.001; Fig. 1B). Furthermore, the rADAMTS-1 (H) group exhibited an increase of ~16% (P<0.05) compared with the $BaCl_2$ group after 1 dpi. A marked improvement in grip strength was observed in the rADAMTS-1 (H) group after 3 dpi, reaching nearly 90% of the NC group's performance (ns) and exceeding the $BaCl_2$ group by 19% (P<0.05) (Fig. 1C). By contrast, during the first 7 days, the $BaCl_2$ group exhibited a decrease of ~20% compared with the NC group (P<0.01). The rADAMTS-1 (H) group exhibited higher grip force values than both the $BaCl_2$ and rADAMTS-1 (L) groups (P<0.01 and <0.5, respectively) (Fig. 1D). At 14 days after muscle damage, the grip force values in the rADAMTS-1 (H) group were similar to those in the NC group. By contrast, decreases of ~10 and 7% were observed in the $BaCl_2$ and rADAMTS-1 (L) groups, respectively (ns; Fig. 1E).

Histological changes were assessed by group based on the time elapsed after $BaCl_2$ injection (Fig. 1F). At 1 dpi, the margins of the TA muscle appeared rounded, with mild infiltration of inflammatory cells in the injured groups. Inflammatory cell infiltration increased at 3 dpi, at which point the myofibers maintained rounded margins and proliferating cells were evident. The presence of centrally located myonuclei, irregularly shaped fibers, and small myofibers at 7 dpi indicates proliferation (25). The rADAMTS-1 (H) group exhibited active proliferation patterns at 7 dpi, with myonuclei mainly located at the center of most muscle fibers at 14 dpi. The TA muscles exhibited angular margins, comparable with those in the NC group, indicating maturation at 14 dpi in both the $BaCl_2$ and rADAMTS-1 groups. The rADAMTS-1 (H) group showed a more extensive proliferative region than the $BaCl_2$ group at 7 and 14 dpi.

Effects of rADAMTS-1 on MuSCs population over time after $BaCl_2$ injury. Research on mouse skeletal muscle has demonstrated that MuSCs can be isolated (26) and are characterized by negative expression of CD45, CD31, and Sca1, and positive expression of VCAM-1 (Fig. 2A). Compared with the NC group, a marked increase in MuSC numbers was observed in all $BaCl_2$-treated groups following muscle injury (Fig. 2B). The temporal pattern indicated a significant increase in MuSC numbers at 3 dpi in all the injured groups, followed by a gradual decline over time (Fig. 2C). At 3 dpi, the number of MuSCs (normalized to NC) in the rADAMTS-1 (H) group was ~4.5-fold higher than that in the NC group (P<0.001) and ~1.2-fold higher than that in the $BaCl_2$ group (P<0.01). At 7 dpi, the rADAMTS-1 (H) group exhibited an ~1.6-fold increase compared with the $BaCl_2$ group (P<0.01). A further decrease was observed in all injured groups at 14 dpi, with the levels remaining ~1.4-fold higher in the high-dose group than in the NC group (ns). Pax7 expression was analyzed throughout the experimental period to assess MuSC abundance (Fig. 2D). Similar to the flow cytometry results, Pax7 expression in the injury group significantly increased at 3 dpi and then decreased over time. The rADAMTS-1 (H) group exhibited 1.3-, 2-, 1.3-, and 1.6-fold higher expression at 1 (ns), 3 (P<0.001), 7 (ns), and 14 (ns) dpi, respectively, than the $BaCl_2$ group, consistently maintaining a slightly higher expression (Fig. 2E).

Effects of rADAMTS-1 on ADAMTS-1, NICD, and Hes-1 expression in TA tissue after $BaCl_2$ injection. The temporal expression patterns of ADAMTS-1, NICD, and Hes-1 were investigated during muscle regeneration following injury by performing western blot analysis at 1, 3, 7, and 14 dpi (Fig. 3A). In the $BaCl_2$-induced muscle injury group, expression levels of ADAMTS-1, NICD, and Hes-1 were notably upregulated at 1 dpi and gradually decreased thereafter. Throughout the experiment, the rADAMTS-1 (H) group consistently showed higher ADAMTS-1 expression (1.2-1.5-fold) compared with the $BaCl_2$ group, with statistically significant differences on days 1 (P<0.01), 3 (P<0.001), 7 (P<0.01), and 14 (P<0.5; Fig. 3B). Within-group comparisons of NICD and Hes-1 levels demonstrated a consistent decrease in the rADAMTS-1 (H) group at all time points (Fig. 3C and D). A supplementary validation experiment confirmed that rADAMTS-1 alone (10 mg/kg) did not change these marker expressions under non-injury conditions (Fig. S5).

Effects of rADAMTS-1 on the expression of myogenic markers in TA tissue. eMyHC expression was examined in all the experimental groups throughout the study period (Fig. 4A). IHC analysis revealed a significant increase in eMyHC-positive muscle fibers at 3 dpi in all groups injected with $BaCl_2$, followed by a subsequent decline over time. Compared with the NC group, all other groups exhibited ~a 15-fold increase in eMyHC expression at 1 dpi (P<0.001) (Fig. 4B). Compared with the $BaCl_2$ group, the rADAMTS-1 (H) group showed significantly higher numbers of eMyHC-positive muscle fibers, with increases of ~1.5-, 2.7- and 3.4-fold at 3 (P<0.05), 7 (P<0.001) and 14 (P<0.01) dpi, respectively (Fig. 4C-E).

Immunofluorescence analysis was conducted at each time point to evaluate MyoD expression in myoblasts in all experimental groups (Fig. 4F). MyoD expression significantly peaked

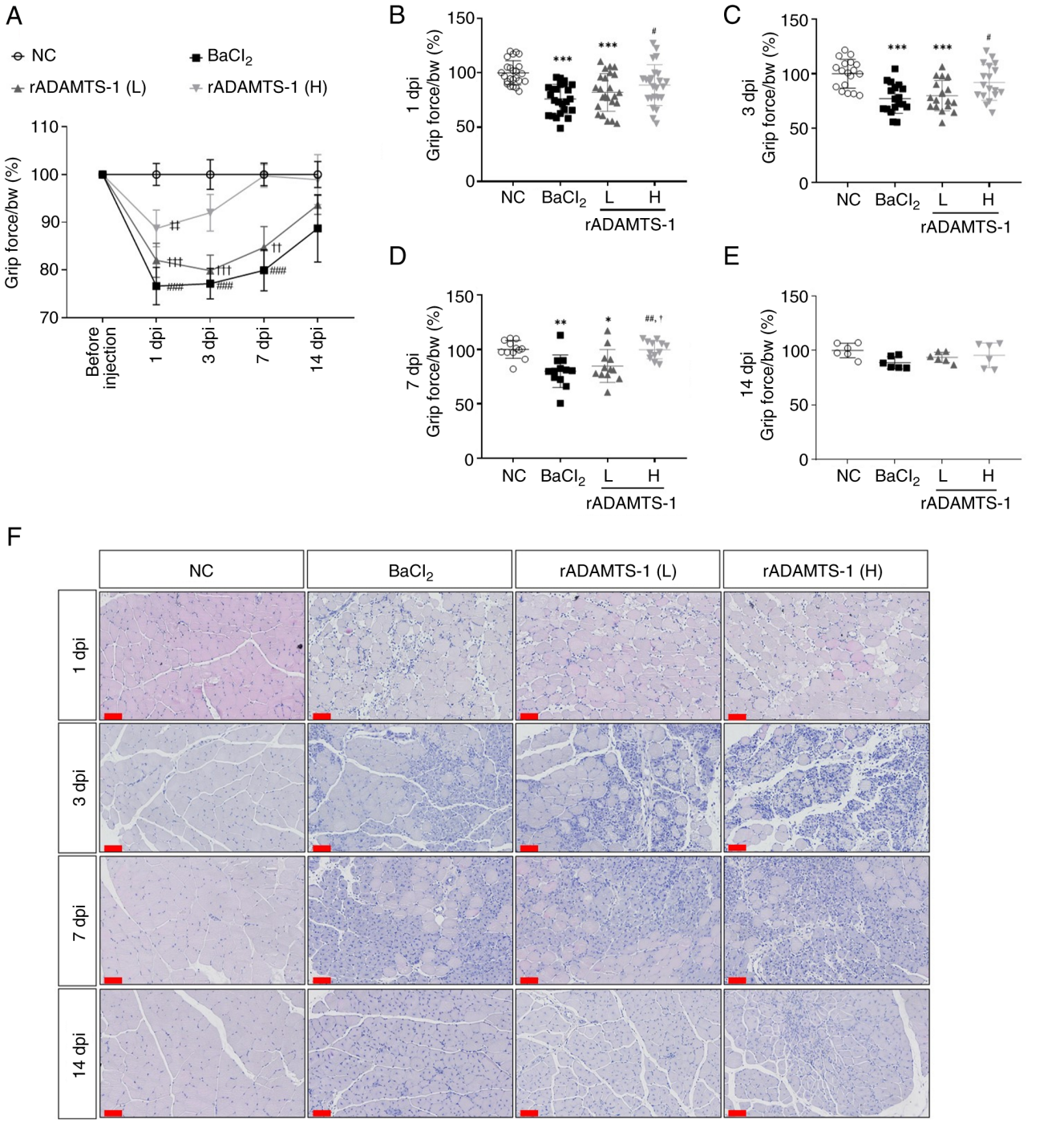

Figure 1. Effects of rADAMTS-1 on recovery following $BaCl_2$-induced TA muscle injury. Groups included NC, $BaCl_2$, rADAMTS-1 treatment groups (L) and (H). Daily intraperitoneal injections of rADAMTS-1 (L) or (H) were initiated immediately after injury and continued until the designated endpoint. (A) Grip strength measurements, normalized to body weight, were recorded throughout the experimental period. Statistical significance was determined using two-way analysis of variance as follows: $^{\#\#\#}$P<0.001 vs. $BaCl_2$ group at day 0; ††P<0.01 and †††P<0.001 vs. rADAMTS-1 (L) at day 0; ‡‡P<0.01 vs. rADAMTS-1 (H) at day 0. (B-E) Grip strength at 1, 3, 7, and 14 dpi. Each dot represents an individual mouse, with error bars indicating the standard deviation. Statistical significance was determined using one-way analysis of variance, followed by Tukey's post hoc test; *P<0.05, **P<0.01 and ***P<0.001 vs. NC group; $^{\#}$P<0.05 and $^{\#\#}$P<0.01 vs. $BaCl_2$ group; †P<0.05 vs. rADAMTS-1 (L). (F) Representative histological images of TA muscle sections stained with hematoxylin and eosin (scale bar, 60 μm) at the corresponding time points. ADAMTS-1, a disintegrin and metalloproteinase with thrombospondin motifs 1; rADAMTS-1, recombinant ADAMTS-1; $BaCl_2$, barium chloride; TA, tibialis anterior; NC, non-injured control; rADAMTS-1 (L), rADAMTS-1 at 5 mg/kg; rADAMTS-1 (H), rADAMTS-1 at 10 mg/kg.

at 3 dpi in the injury group and then gradually declined, which was consistent with the IHC results. The rADAMTS-1 (H) group consistently demonstrated elevated MyoD expression compared with the $BaCl_2$ group, with fold increases of 1.3 (ns), 2.3 (P<0.01), 1.7 (ns), and 3.7 (ns) at 1, 3, 7, and 14 dpi, respectively (Fig. 4G).

Effects of rADAMTS-1 on myogenic regulatory transcription factors in TA tissue after $BaCl_2$-induced injury. MyoD and MyoG expression peaked at 3 dpi and then gradually decreased (Fig. 5A). On day 14, MyoD levels had significantly decreased ~12-fold compared with day 3, and 7-fold

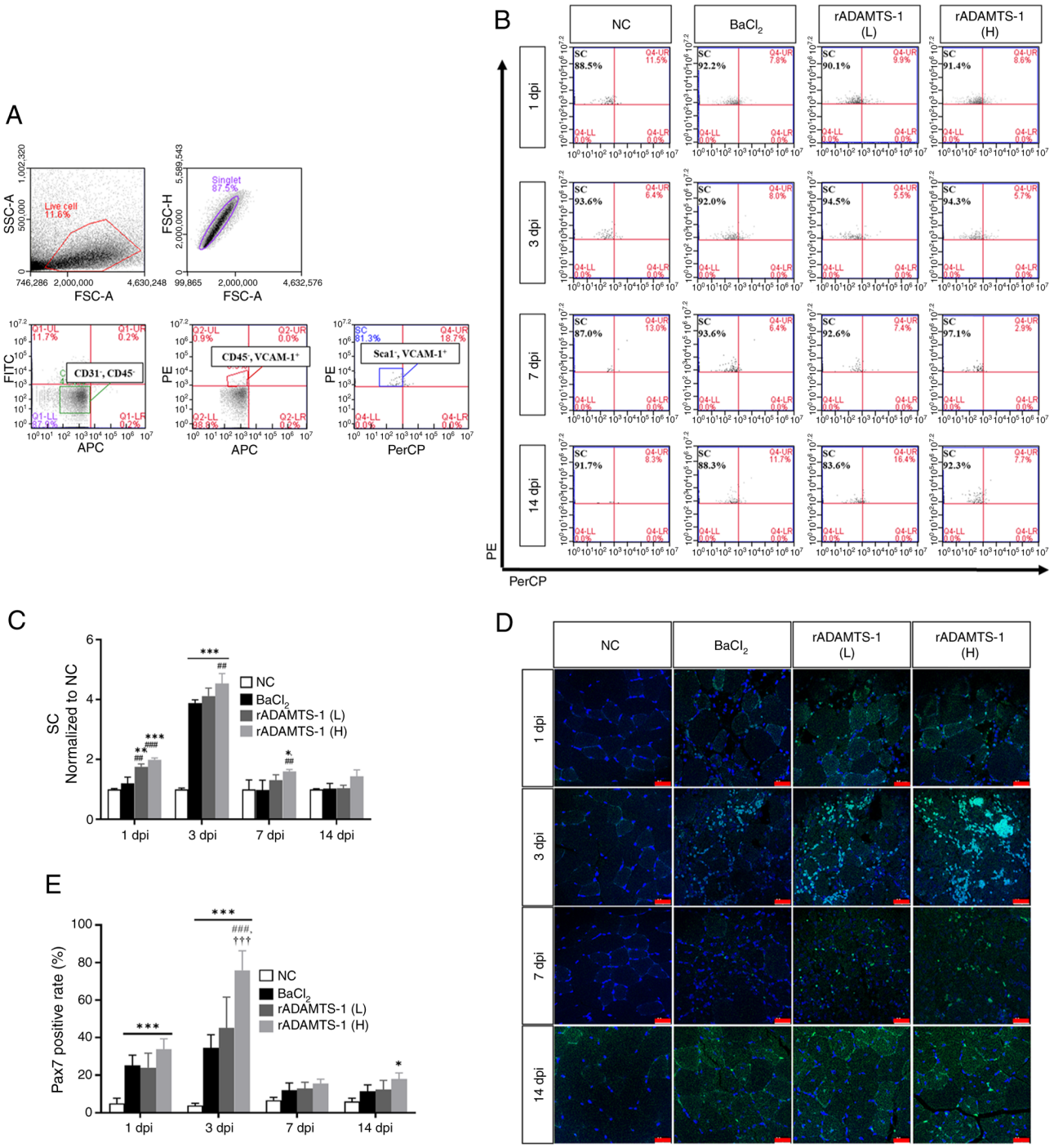

Figure 2. Effect of rADAMTS-1 on MuSCs following $BaCl_2$-induced TA muscle injury. Groups included NC, $BaCl_2$, and two treatment groups receiving rADAMTS-1 (L) and (H). Daily intraperitoneal injections of rADAMTS-1 were initiated immediately after injury and continued until the designated time point for analysis. (A) Flow cytometry analysis of MuSCs isolated from injured TA muscles, defined by surface marker expression ($CD45^-/CD31^-/Sca1^-/VCAM1^+$). (B) Representative gating strategy for MuSCs across experimental groups at different time points. (C) Relative number of MuSCs normalized to the NC group over time. Statistical significance was determined using one-way analysis of variance, followed by Tukey's post hoc test: $^*P<0.05$, $^{**}P<0.01$ and $^{***}P<0.001$ vs. NC; $^{\#\#}P<0.01$ and $^{\#\#\#}P<0.001$ vs. $BaCl_2$ group. (D) Representative immunofluorescence images of $Pax7^+$ cells in injured TA muscle at different time points (scale bar, 25 μm). (E) Quantification of $Pax7^+$ cell percentages over time. Statistical significance was determined using one-way analysis of variance with Tukey's post hoc test: $^*P<0.05$ and $^{***}P<0.001$ vs. NC; $^{\#\#\#}P<0.001$ vs. $BaCl_2$; $^{\dagger\dagger\dagger}P<0.001$ vs. rADAMTS-1 (L). ADAMTS-1, a disintegrin and metalloproteinase with thrombospondin motifs 1; rADAMTS-1, recombinant ADAMTS-1; MuSCs, skeletal muscle satellite cells; $BaCl_2$, barium chloride; TA, tibialis anterior; NC, non-injured control; rADAMTS-1 (L), rADAMTS-1 at 5 mg/kg; rADAMTS-1 (H), rADAMTS-1 at 10 mg/kg; CD, cluster of differentiation; Sca1, stem cell antigen 1; VCAM1, vascular cell adhesion molecule; Pax7, paired box protein.

compared with day 7 ($P<0.001$ for both). MyoG expression also significantly declined (~2-fold) compared with day 3 ($P<0.01$), whereas the decrease compared with day 7 (1.4-fold) was not statistically significant (ns). Comparative analysis of western blot data over the same timeframe consistently revealed the highest expression levels of MyoD and MyoG in the high-dose rADAMTS-1 (H) group (Fig. 5B and C). On days 7 and 14, the rADAMTS-1 (L) and (H)

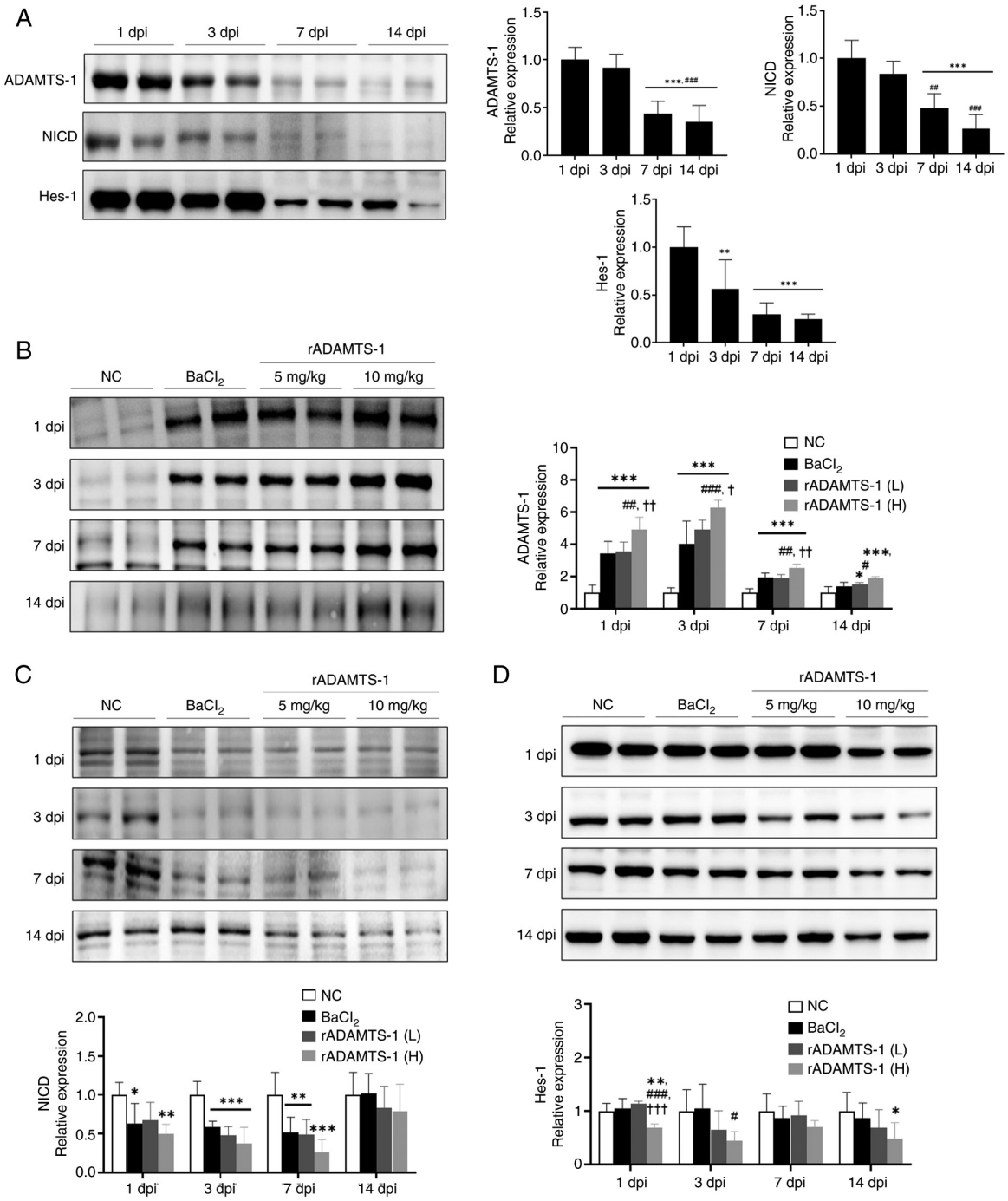

Figure 3. Effects of rADAMTS-1 on the expression of ADAMTS-1-associated markers in $BaCl_2$-injured TA muscle. Groups included NC, $BaCl_2$, rADAMTS-1 treatment groups (L), and (H). Daily intraperitoneal injections of rADAMTS-1 were initiated immediately after injury and continued until the designated time point for analysis. (A) Temporal expression patterns of ADAMTS-1, NICD, and Hes-1 in the NC and $BaCl_2$ groups at 1, 3, 7, and 14 days post-injury (dpi). Comparative expression levels of (B) ADAMTS-1, (C) NICD, and (D) Hes-1 among treatment groups [NC, $BaCl_2$, rADAMTS-1 (L), and rADAMTS-1 (H)] at each time point. Mice received daily intraperitoneal injections of rADAMTS-1 until the designated dpi. Each data point represents an individual biological replicate; error bars indicate standard deviation. Statistical significance in panels (A) was determined using one-way analysis of variance, followed by Tukey's honestly significant difference *post hoc* test, as indicated as follows: **P<0.01 and ***P<0.001 vs. 1 dpi; $^{\#\#}$P<0.01 and $^{\#\#\#}$P<0.001 vs. 3 dpi. For panels (B-D), statistical comparisons were made using one-way analysis of variance with Tukey's post hoc test: *P<0.05, **P<0.01 and ***P<0.001 vs. NC; $^{\#}$P<0.05 $^{\#\#}$P<0.01 and $^{\#\#\#}$P<0.001 vs. $BaCl_2$; †P<0.05, ††P<0.01 and †††P<0.001 vs. rADAMTS-1 (L). ADAMTS-1, a disintegrin and metalloproteinase with thrombospondin motifs 1; rADAMTS-1, recombinant ADAMTS-1; $BaCl_2$, barium chloride; TA, tibialis anterior; NC, non-injured control; rADAMTS-1 (L), rADAMTS-1 at 5 mg/kg; rADAMTS-1 (H), rADAMTS-1 at 10 mg/kg; NICD, Notch intracellular domain; Hes-1, hairy and enhancer of split-1; dpi, days post-injury.

treatment groups exhibited increased MyoG expression compared with the $BaCl_2$ group. A supplementary validation experiment confirmed that rADAMTS-1 alone (10 mg/kg) did not alter myogenic marker expression under non-injury conditions (Fig. S5).

Effect of rADAMTS-1 on the proliferation and differentiation stage of myogenesis in vitro. Primary skeletal muscle cells were treated with rADAMTS-1, followed by a BrdU assay to investigate its role in skeletal muscle cell activation (Fig. 6A). Activation increased in a concentration-dependent

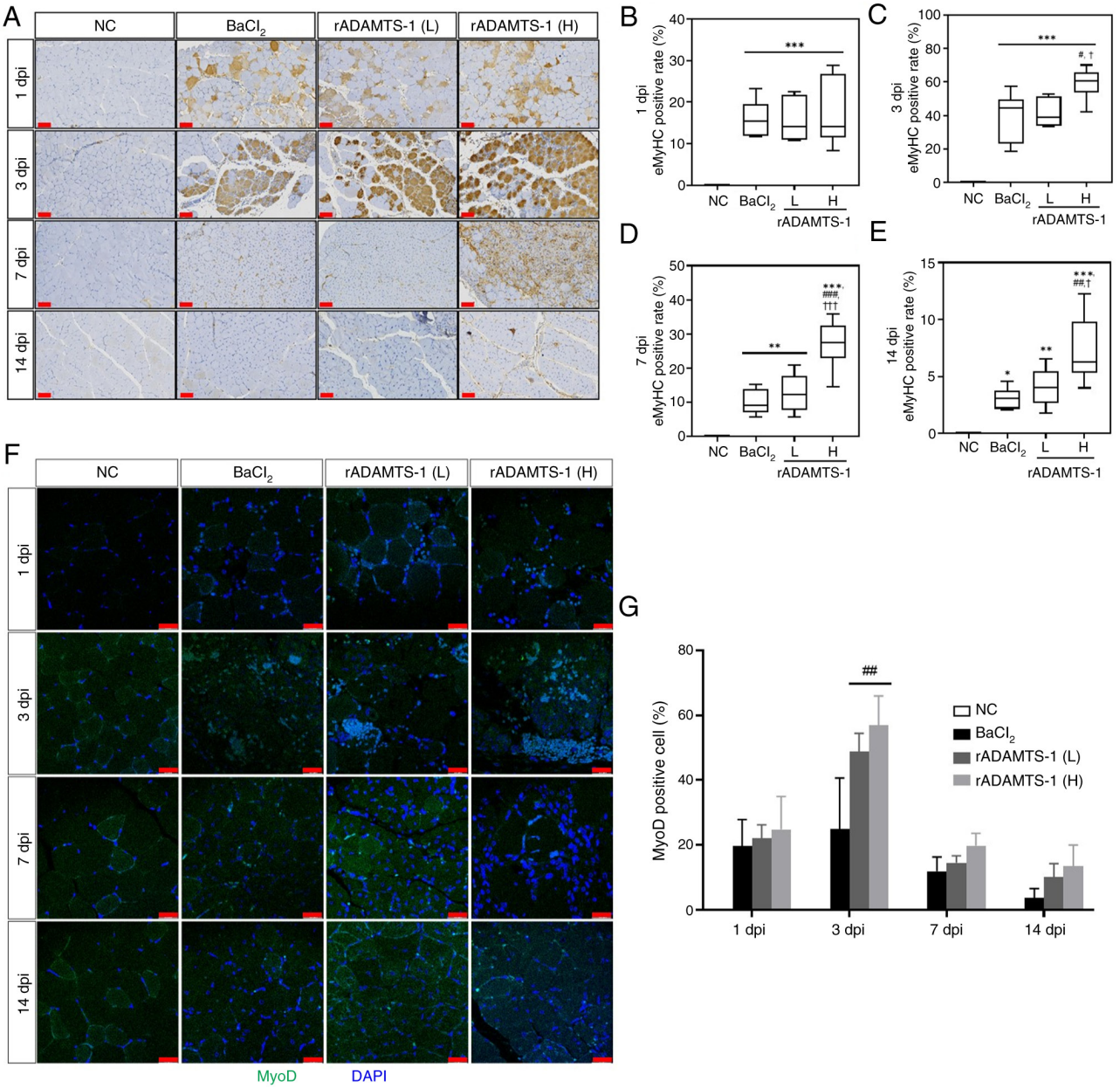

Figure 4. Effects of rADAMTS-1 on muscle regeneration markers in $BaCl_2$-injured TA muscle. Groups included NC, $BaCl_2$, rADAMTS-1 treatment groups (L), and (H). Daily intraperitoneal injections were given starting immediately after injury and maintained until the designated analysis point. (A) Representative immunohistochemical staining of eMyHC in injured TA muscles treated with rADAMTS-1 at 1, 3, 7, and 14 days dpi (scale bar, 60 μm). (B-E) Quantification was performed using image analysis software to assess the eMyHC-positive area at each time point. (F) Representative immunofluorescence images of MyoD-positive cells in injured TA muscle (scale bar, 25 μm) treated with rADAMTS-1 at 1, 3, 7, and 14 dpi. (G) Quantification of MyoD-positive cell percentages over time across groups. All data are presented as mean ± standard deviation. Statistical significance was determined using one-way analysis of variance, followed by Tukey's post hoc test: *P<0.05, **P<0.01 and ***P<0.001 vs. NC group; $^{\#}$P<0.05 $^{\#\#}$P<0.01 and $^{\#\#\#}$P<0.001 vs. $BaCl_2$ group; †P<0.05 and †††P<0.001 vs. rADAMTS-1 (L) group. ADAMTS-1, a disintegrin and metalloproteinase with thrombospondin motifs 1; rADAMTS-1, recombinant ADAMTS-1; $BaCl_2$, barium chloride; TA, tibialis anterior; NC, non-injured control; rADAMTS-1 (L), rADAMTS-1 at 5 mg/kg; rADAMTS-1 (H), rADAMTS-1 at 10 mg/kg; eMyHC, embryonic myosin heavy chain; dpi, days post-injury; MyoD, myoblast determination protein 1; dpi, days post-injury.

manner, with treatment at 10 ng/ml rADAMTS-1 producing a significant 1.4-fold increase compared with the control (Con) group (P<0.5). The effects of rADAMTS-1 on primary skeletal muscle cell differentiation were investigated (Fig. 6B). The myotube length increased in a dose-dependent manner, and treatment with 10 ng/ml rADAMTS-1 resulted in an ~2.5-fold increase compared with the Con group (P<0.001). rADAMTS-1 treatment also significantly increased the expression of myogenic markers. MyoD and MyoG levels elevated ~2- and 3.5-fold, respectively, compared with those in the Con group (P<0.05; Fig. 6C). In addition, ADAMTS-1 expression level increased ~2-fold in the rADAMTS-1-treated group, whereas NICD and Hes-1 expression levels were ~0.6-fold and 0.7-fold lower, respectively, than in the Con group (P<0.01).

Effects of rADAMTS-1 on myogenesis-related genes in vitro. RNA-seq analysis was performed to identify differentially expressed genes in response to rADAMTS-1 treatment during muscle cell differentiation. A total of 3,185 differentially

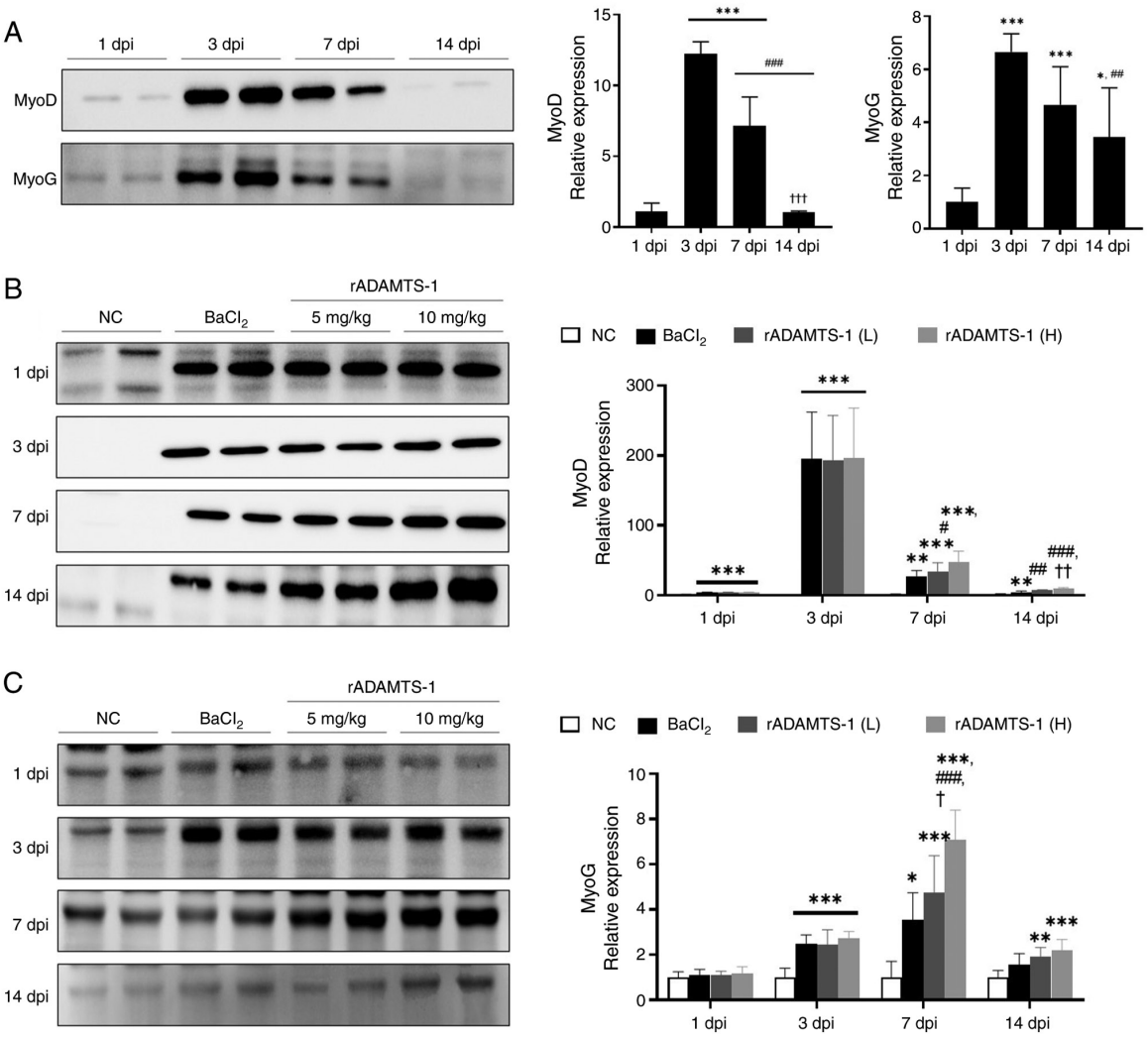

Figure 5. Effects of rADAMTS-1 on early myogenic markers in $BaCl_2$-injured TA muscle. Groups included NC, $BaCl_2$, rADAMTS-1 treatment groups (L), and (H). Daily intraperitoneal injections of rADAMTS-1 were administered at two doses starting immediately after injury and continuing until the designated time point of analysis. Temporal expression of (A) MyoD and MyoG in the injured TA at 1, 3, 7, and 14 dpi. Comparative expression of (B) MyoD and (C) MyoG across experimental groups at each time point. Each data point represents an individual replicate; error bars indicate standard deviation. Statistical significance in (A) was determined using one-way analysis of variance, followed by Tukey's post hoc test and is indicated as follows: *P<0.05 and ***P<0.001 vs. 1 dpi; $^{\#\#}$P<0.01 and $^{\#\#\#}$P<0.001 vs. 3 dpi; †††P<0.001 vs. 7 dpi. Statistical significance in (B) and (C) is indicated as follows: *P<0.05, **P<0.01 and ***P<0.001 vs. the NC group; $^{\#}$P<0.05 $^{\#\#}$P<0.01 and $^{\#\#\#}$P<0.001 vs. the $BaCl_2$ group; †P<0.05 and ††P<0.01 vs. the rADAMTS-1 (L) group. ADAMTS-1, a disintegrin and metalloproteinase with thrombospondin motifs 1; rADAMTS-1, recombinant ADAMTS-1; $BaCl_2$, barium chloride; TA, tibialis anterior; NC, non-injured control; rADAMTS-1 (L), rADAMTS-1 at 5 mg/kg; rADAMTS-1 (H), rADAMTS-1 at 10 mg/kg; MyoD, myoblast determination protein 1; MyoG, myogenin; dpi, days post-injury.

expressed genes (P<0.05), including 1,959 upregulated and 1,226 downregulated genes. Genes encoding skeletal muscle-associated factors, such as *Myh1*, *Myh2*, *Myh4*, *Myf6* and *Mymx*, were significantly upregulated following rADAMTS-1 treatment (Fig. 7A), and qPCR validation confirmed these increases compared with the Con group (Fig. 7B).

Gene Ontology (GO) enrichment analysis revealed that rADAMTS-1 promoted the expression of genes involved in myogenic differentiation and contractile apparatus formation. In the biological process category, 25% of the top 20 enriched terms were related to muscle development and regeneration, including 'organelle fission,' 'nuclear division,' 'muscle cell differentiation' and 'muscle system process' (Fig. 7C). This pattern suggested that rADAMTS-1 facilitates the transcriptional activation of myogenic programs that drive myotube maturation.

In the cellular component category, enrichment of 'extracellular matrix,' 'external encapsulating structure,' 'actin cytoskeleton,' 'collagen-containing extracellular matrix,' 'contractile fiber' and 'myofibril' indicated coordinated remodeling of extracellular and cytoskeletal structures (Fig. 7D). Such enrichment implied that rADAMTS-1 not only enhanced myogenic gene expression but may also contribute to structural organization and matrix remodeling during differentiation.

Molecular function analysis highlighted genes involved in 'actin filament binding,' 'cytoskeletal motor activity' and 'growth factor binding' (Fig. 7E). These functional groups suggest enhanced cytoskeletal dynamics and intracellular signaling, which are critical for myoblast fusion and alignment during myotube formation.

Consistently, differentiated C2C12 cells showed increased myotube formation in the rADAMTS-1 treated group (Fig. S6),

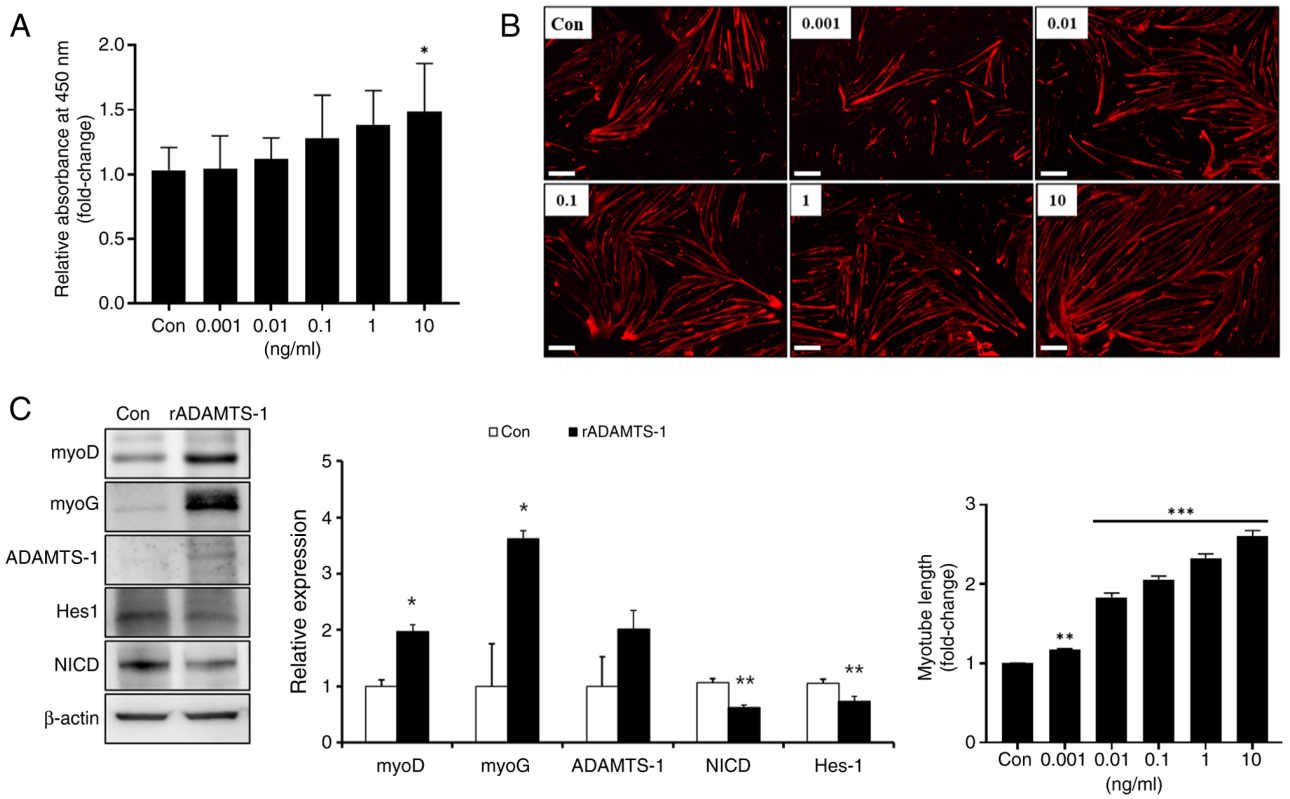

Figure 6. Effects of rADAMTS-1 on proliferation and differentiation of primary skeletal muscle cells. (A) Dose-dependent proliferative effects of rADAMTS-1 (0.001-10 ng/ml) on primary skeletal muscle cells, assessed using the bromodeoxyuridine assay. (B) Dose-dependent effect of rADAMTS-1 (0.001-10 ng/ml) on the differentiation of primary skeletal muscle cells. Quantification of myotube length following differentiation (scale bar, 200 μm). (C) Western blot analysis showing the expression of myogenic and ADAMTS-1 related markers (MyoD, MyoG, ADAMTS-1, NICD, Hes-1, and β-actin) following rADAMTS-1 treatment at a concentration of 10 ng/ml, indicating its promotion of early-stage myogenic differentiation through inhibition of NICD signaling. Each data point represents an individual measurement; error bars indicate standard deviation. Statistical significance was determined using one-way analysis of variance followed by Tukey's honestly significant difference *post hoc* test and is indicated as follows: (A) *P<0.05 vs. Con group; (B) **P<0.01 and ***P<0.001 vs. Con group; (C) *P<0.05 and **P<0.01 vs. Con group. ADAMTS-1, a disintegrin and metalloproteinase with thrombospondin motifs 1; rADAMTS-1, recombinant ADAMTS-1; MyoD, myoblast determination protein 1; MyoG, myogenin; NICD, Notch intracellular domain; HES-1, hairy and enhancer of split-1; Con, control.

supporting the transcriptomic results of enhanced myogenic differentiation.

Discussion

With the rapidly aging global population, the need for effective therapies targeting sarcopenia has become increasingly urgent (27). The present study evaluated the therapeutic potential of rADAMTS-1 in promoting muscle regeneration. The results suggested that rADAMTS-1 promoted MuSC activation and differentiation, potentially counteracting the age-related decline in regenerative capacity. In addition, rADAMTS-1 sustained the expression of myogenic factors over time, indicating possible long-term benefits for restoring compromised regenerative mechanisms in older adults.

To assess these effects *in vivo*, a $BaCl_2$-induced muscle injury model was used. Compared with the $BaCl_2$ group, the rADAMTS-1 (H) group exhibited significantly improved functional recovery, as indicated by enhanced grip strength and sustained histological evidence of muscle regeneration up to 14 dpi. Flow cytometry and immunofluorescence analyses revealed a significant increase in MuSC numbers at 3 dpi in all $BaCl_2$-injected groups, although these numbers decreased over time. Specifically, the rADAMTS-1 (H) group showed a marked increase in MuSCs at 3 dpi. Despite a gradual reduction over time, MuSC levels in this group remained significantly higher than those in the other groups through 14 dpi. This sustained increase in MuSCs likely facilitates prolonged proliferative activity prior to differentiation, thereby contributing to effective regeneration (10,28,29).

In parallel, downstream indicators of regeneration, including eMyHC and MyoD expression, were assessed. The expression pattern of eMyHC, an early marker of muscle regeneration (20), closely mirrored the abundance of MuSCs. MyoD, a transcription factor guiding MuSCs toward the skeletal muscle lineage (30), also showed sustained expression. eMyHC and MyoD levels were both significantly elevated in the rADAMTS-1 (H) group at 3 dpi and remained higher than those in the other groups through 14 dpi, despite eMyHC being classified as an early-phase marker (31). These results suggest that rADAMTS-1-induced MuSC expansion, coupled with suppressed Notch signaling, contributes to prolonged regenerative activity.

Although the results demonstrated reduced NICD and Hes-1 levels following rADAMTS-1 treatment, these observations are associative and did not establish a direct causal link between rADAMTS-1 and Notch inhibition. Downregulation of Notch signaling leads to upregulation of MyoD and promotes myogenic differentiation (32). Activation of NICD or RBP-J represses MyoD transcription by interacting with its basic helix-loop-helix domain (33,34). Given this established

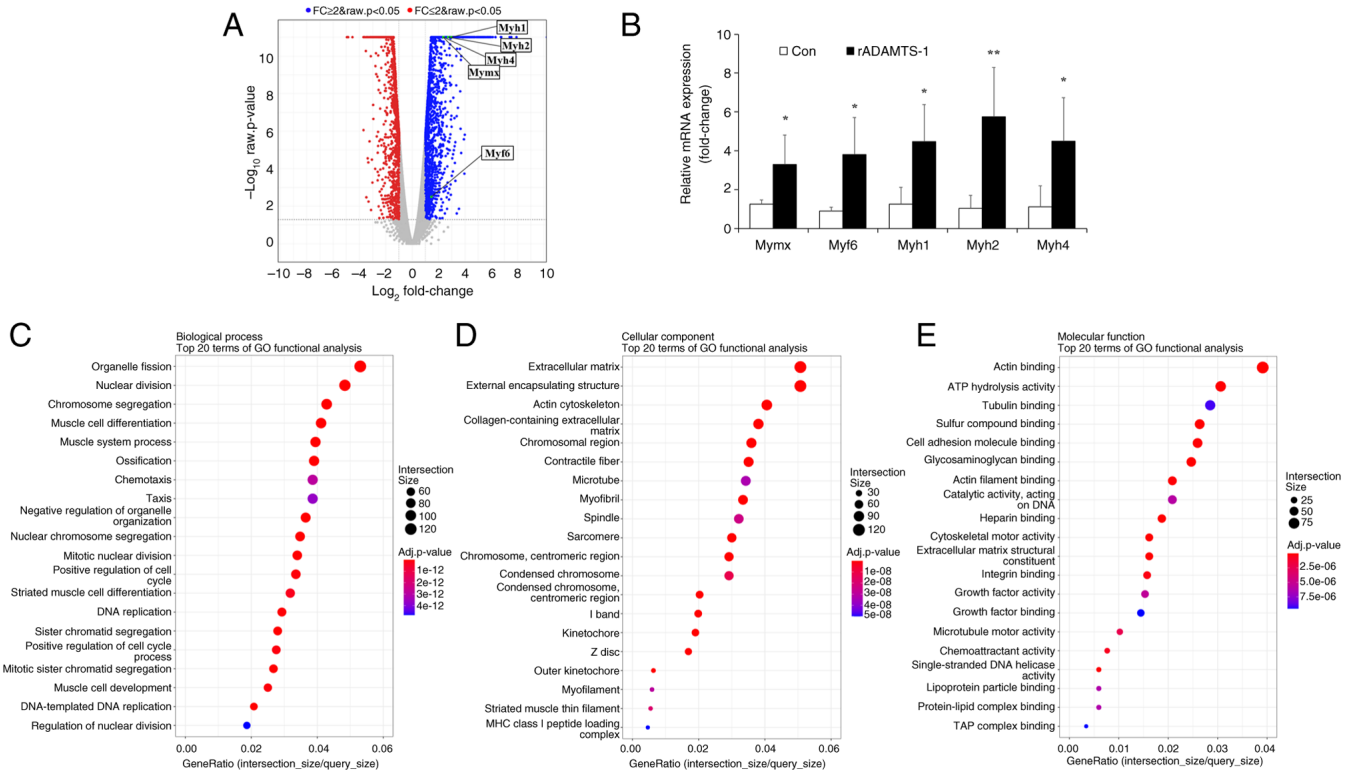

Figure 7. Transcriptomic analysis and GO enrichment of muscle cell differentiation following rADAMTS-1 treatment. C2C12 cells were treated with 10 ng/ml rADAMTS-1 and differentiated for 3 days before RNA-seq analysis. (A) Volcano plot showing DEGs. Blue and red dots indicate significantly upregulated and downregulated DEGs, respectively. (B) Validation of selected DEGs from RNA-sequencing by quantitative PCR. Results are presented as mean ± SD. Statistical significance was determined using one-way analysis of variance with Tukey's post hoc test and is indicated as follows: *P<0.05 and **P<0.01 vs. the control group. GO enrichment analysis of the top 20 terms associated with (C) Biological Process, (D) Cellular Component and (E) Molecular Function, based on the identified DEGs. GO, Gene Ontology; ADAMTS-1, a disintegrin and metalloproteinase with thrombospondin motifs 1; rADAMTS-1, recombinant ADAMTS-1; RNA-seq, RNA sequencing; DEG, differentially expressed genes.

inhibitory relationship, the decrease in NICD and Hes-1 expression and the increase in MyoD and MyoG observed in the present study suggested that rADAMTS-1 facilitates muscle regeneration by attenuating Notch signaling activity rather than by directly cleaving Notch components.

Recent evidence from a study by Lee *et al* (13) demonstrated that rADAMTS-1 directly binds to Notch1 and inhibits ADAM10-mediated S2 cleavage within its extracellular TMIC domain. This proteolytic regulation prevents the release of the active NICD, thereby downregulating Hes-1 expression and promoting myogenic differentiation (11). In agreement with this mechanism, the present data showed reduced NICD and Hes-1 levels in rADAMTS-1-treated muscles, supporting that rADAMTS-1 can negatively regulate Notch signaling through its metalloproteinase activity.

Myogenic differentiation was further examined by analyzing MyoG expression. MyoD-positive precursor cells differentiate and fuse to restore damaged muscle fibers (35), while MyoG triggers the final stages of myogenic differentiation (36). As myofibers mature, MyoG expression typically decreases (37). In the $BaCl_2$-treated group, both MyoD and MyoG peaked at 3 dpi and declined thereafter. However, the rADAMTS-1 (H) group exhibited sustained expression of both factors at 7 and 14 dpi, indicating a prolonged activation of the myogenic program. These results are consistent with those reported by Du *et al* (11), who observed that ADAMTS-1 influences the persistent MuSC activation.

To validate these findings *in vitro*, primary skeletal muscle cells were treated with rADAMTS-1. These cells were selected for their close resemblance to MuSCs in terms of myogenic potential and regenerative capacity (38). rADAMTS-1 treatment suppressed NICD expression and upregulated MyoD and MyoG, mirroring the *in vivo* results. These findings suggested that rADAMTS-1 exerts a sustained effect on early myogenic differentiation by modulating key regulatory proteins involved in myoblast commitment. In particular, the findings from human primary skeletal muscle cells support the translational relevance of rADAMTS-1, indicating that its myogenic effects are potentially applicable to human muscle regeneration. To further explore the transcriptional landscape associated with rADAMTS-1 treatment, RNA-seq analysis was conducted using the C2C12 myoblast cell line, a reproducible and widely used *in vitro* model for transcriptomic studies (39,40). rADAMTS-1 treatment upregulated myogenic genes, such as *Myh* and *Mymx*. *Myh* is associated with muscle contractility and cellular motility (41), while *Mymx* plays a key role in myoblast fusion during muscle regeneration and organ development (42). In addition, *Myf6*, a transcription factor essential for maintaining the MuSC pool by inhibiting premature differentiation, was upregulated (43). These RNA-seq findings, confirmed by qPCR, indicate that rADAMTS-1 activates a transcriptional program that supports muscle development and maintenance. GO enrichment analysis further revealed significant activation of pathways involved in muscle cell

differentiation and extracellular matrix (ECM) organization, suggesting that rADAMTS-1 may contribute to an ECM remodeling during muscle regeneration. Taken together with its metalloproteinase-mediated regulation of Notch signaling, these data indicate that rADAMTS-1 enhances muscle regeneration through dual modulation.

In a supplementary validation study, rADAMTS-1 administration alone (10 mg/kg) did not induce significant changes in myogenic marker expression compared with the NC group These findings suggested that rADAMTS-1 does not activate myogenic processes under normal conditions, but rather facilitates regeneration during muscle differentiation. It is consistent with previous reports indicating that ADAMTS-1 primarily modulates the extracellular microenvironment during regenerative conditions rather than in intact tissue (11,44). As rADAMTS-1 administration alone did not cause detectable changes in muscles or systemic conditions, this group was not included in the main experimental design.

As ADAMTS family proteins can modulate extracellular matrix turnover, and excessive activity may theoretically lead to fibrosis, inflammation, or ECM degradation. However, no abnormal histological findings, inflammatory infiltration, or fibrotic changes were observed in any of the rADAMTS-1 treated groups during the 14-day observation period, suggesting that rADAMTS-1 does not elicit overt toxicity under the conditions tested. Additionally, time-dependent plasma concentration analysis confirmed systemic absorption of rADAMTS-1 following IP administration.

The present study has clear methodological limitations that should be acknowledged. Only male mice were used, following most previous studies employing the $BaCl_2$-induced skeletal muscle injury model (45-47). Although this approach minimizes biological variability and ensures experimental consistency, it inevitably limits the generalizability of the results, as potential sex-dependent differences could not be evaluated. Another important limitation lies in the use of the $BaCl_2$-induced acute injury model rather than a chronic or age-related paradigm. This model provides a reproducible and temporally defined framework for assessing MuSC-driven regeneration but does not fully capture the chronic and multifactorial pathophysiology of sarcopenia (48). While an aging model would have offered greater physiological relevance, it could not be implemented within the scope and timeframe of the present study. Moreover, naturally aged rodents are known to exhibit variable manifestations of muscle mass and functional decline depending on strain, sex, and environmental conditions (49,50), suggesting that chronological aging alone may not reliably reproduce the human sarcopenia phenotype. Thus, the $BaCl_2$ model should be regarded as a mechanistic surrogate rather than a direct model of age-related muscle degeneration. Although the RNA-seq analysis and validation were performed using the well-established C2C12 myoblast cell line (51), this represents another limitation of the study, as the results were not verified using *in vivo* samples. Future study will need on regenerated muscle tissues to validate the key RNA-seq-identified genes *in vivo*. The study also focused exclusively on the early phase of muscle repair, emphasizing MuSC activation and early regenerative events. Although this phase represents a critical window for effective regeneration, long-term outcomes such as sustained muscle function and structural remodeling were not addressed. These limitations collectively indicate that additional studies using senescence-accelerated mice or naturally aged models will be essential to validate the long-term efficacy and translational potential of rADAMTS-1 under physiological aging conditions.

In conclusion, rADAMTS-1 enhances muscle regeneration by activating MuSCs and upregulating myogenic factors, thereby driving the expression of genes essential for muscle development. Given the clinical challenges posed by sarcopenia, rADAMTS-1 represents a promising therapeutic candidate for mitigating muscle loss in older adults. Its ability to promote MuSCs proliferation and differentiation, potentially overcoming some limitations of current MuSCs transplantation strategies. Overall, The present study highlighted the potential of rADAMTS-1 for sarcopenia treatment, although further research is needed to confirm its long-term efficacy, safety, and clinical applicability.

Acknowledgements

Not applicable.

Funding

The present study was supported by the Korea Drug Development Fund, funded by the Ministry of Science and ICT, the Ministry of Trade, Industry, and Energy, and the Ministry of Health and Welfare (grant no. RS-2022-00165803).

Availability of data and materials

The RNA-sequencing dataset in the present study may be found in the Zenodo database under accession number DOI: 10.5281/zenodo.17579631 or at the following URL: https://zenodo.org/records/17579631. Other data generated in the present study are included in the figures of this article.

Authors' contributions

JHK was responsible for investigation, methodology, formal analysis and writing the original draft. SHL was responsible for investigation, methodology, formal analysis and resources. SYK investigation, methodology and resources. JWKim, JSJ, EHC, SHL and CYK were responsible for investigation and methodology. BKC was responsible for conceptualization and resources. JWKo and TWK were responsible for conceptualization, project administration, supervision, writing, reviewing and editing. JWKo and TWK confirm the authenticity of all the raw data. All authors read and approved the final manuscript.

Ethics approval and consent to participate

All the experimental procedures were reviewed and approved by the Chungnam National University Animal Care and Use Committee (202310A-CNU-169).

Patient consent for publication

Not applicable.

Competing interests

The authors declare that they have no competing interests.

References

1. Tournadre A, Vial G, Capel F, Soubrier M and Boirie Y: Sarcopenia. Joint Bone Spine 86: 309-314, 2019.
2. Larsson L, Degens H, Li M, Salviati L, Lee YI, Thompson W, Kirkland JL and Sandri M: Sarcopenia: Aging-related loss of muscle mass and function. Physiol Rev 99: 427-511, 2019.
3. Cruz-Jentoft AJ and Sayer AA: Sarcopenia. Lancet 393: 2636-2646, 2019.
4. Petrocelli JJ, Mahmassani ZS, Fix DK, Montgomery JA, Reidy PT, McKenzie AI, de Hart NM, Ferrara PJ, Kelley JJ, Eshima H, *et al*: Metformin and leucine increase satellite cells and collagen remodeling during disuse and recovery in aged muscle. FASEB J 35: e21862. 2021.
5. Kim HJ, Jung DW and Williams DR: Age is just a number: Progress and obstacles in the discovery of new candidate drugs for sarcopenia. Cells 12: 2608, 2023.
6. Huo F, Liu Q and Liu H: Contribution of muscle satellite cells to sarcopenia. Front Physiol 13: 892749, 2022.
7. Schmidt M, Schüler SC, Hüttner SS, von Eyss B and von Maltzahn J: Adult stem cells at work: Regenerating skeletal muscle. Cell Mol Life Sci 76: 2559-2570, 2019.
8. Haroon M, Boers HE, Bakker AD, Bloks NGC, Hoogaars WMH, Giordani L, Musters RJP, Deldicque L, Koppo K, Le Grand F, *et al*: Reduced growth rate of aged muscle stem cells is associated with impaired mechanosensitivity. Aging (Albany NY) 14: 28-53, 2022.
9. Qazi TH, Duda GN, Ort MJ, Perka C, Geissler S and Winkler T: Cell therapy to improve regeneration of skeletal muscle injuries. J Cachexia Sarcopenia Muscle 10: 501-516, 2019.
10. Judson RN and Rossi FMV: Towards stem cell therapies for skeletal muscle repair. NPJ Regen Med 5: 10, 2020.
11. Du H, Shih CH, Wosczyna MN, Mueller AA, Cho J, Aggarwal A, Rando TA and Feldman BJ: Macrophage-released ADAMTS1 promotes muscle stem cell activation. Nat Commun 8: 669, 2017.
12. Mourikis P, Sambasivan R, Castel D, Rocheteau P, Bizzarro V and Tajbakhsh S: A critical requirement for notch signaling in maintenance of the quiescent skeletal muscle stem cell state. Stem Cells 30: 243-252, 2012.
13. Lee SH, Kim SY, Gwon YG, Lee C, Cho IH, Kim TW and Choi BK: Recombinant ADAMTS1 promotes muscle cell differentiation and alleviates muscle atrophy by repressing NOTCH1. BMB Rep 57: 539-545, 2024.
14. Tarum J, Degens H, Turner MD, Stewart C, Sale C and Santos L: Modelling skeletal muscle ageing and repair in vitro. J Tissue Eng Regen Med 2023: 9802235, 2023.
15. Pawlikowski B, Betta ND, Antwine T and Olwin BB: Skeletal muscle stem cell self-renewal and differentiation kinetics revealed by EdU lineage tracing during regeneration. bioRxiv: doi: https://doi.org/10.1101/627851.
16. Al Shoyaib A, Archie SR and Karamyan VT: Intraperitoneal route of drug administration: Should it be used in experimental animal studies?. Pharm Res 37: 12, 2019.
17. Ibraheem D, Elaissari A and Fessi H: Administration strategies for proteins and peptides. Int J Pharm 477: 578-589, 2014.
18. Takeshita H, Yamamoto K, Nozato S, Inagaki T, Tsuchimochi H, Shirai M, Yamamoto R, Imaizumi Y, Hongyo K, Yokoyama S, *et al*: Modified forelimb grip strength test detects aging-associated physiological decline in skeletal muscle function in male mice. Sci Rep 7: 42323, 2017.
19. Ghaibour K, Rizk J, Ebel C, Ye T, Philipps M, Schreiber V, Metzger D and Duteil D: An efficient protocol for CUT&RUN analysis of FACS-isolated mouse satellite cells. J Vis Exp 197: e65215, 2023.
20. Gilda JE and Gomes AV: Stain-Free total protein staining is a superior loading control to β-actin for Western blots. Anal Biochem 440: 186-188, 2013.
21. Fortes MA, Marzuca-Nassr GN, Vitzel KF, da Justa Pinheiro CH, Newsholme P and Curi R: Housekeeping proteins: How useful are they in skeletal muscle diabetes studies and muscle hypertrophy models?. Anal Biochem 504: 38-40, 2016.
22. Paul RG, Hennebry AS, Elston MS, Conaglen JV and McMahon CD: Regulation of murine skeletal muscle growth by STAT5B is age- and sex-specific. Skelet Muscle 9: 19, 2019.
23. Wang R, Kumar B, Doud EH, Mosley AL, Alexander MS, Kunkel LM and Nakshatri H: Skeletal muscle-specific overexpression of miR-486 limits mammary tumor-induced skeletal muscle functional limitations. Mol Ther Nucleic Acids 28: 231-248, 2022.
24. Livak KJ and Schmittgen TD: Analysis of relative gene expression data using real-time quantitative PCR and the 2(-Delta Delta C(T)) Method. Methods 25: 402-408, 2001.
25. Forcina L, Cosentino M and Musarò A: Mechanisms regulating muscle regeneration: Insights into the interrelated and time-dependent phases of tissue healing. Cells 9: 1297, 2020.
26. Choo HJ, Canner JP, Vest KE, Thompson Z and Pavlath GK: A tale of two niches: Differential functions for VCAM-1 in satellite cells under basal and injured conditions. Am J Physiol Cell Physiol 313: C392-C404, 2017.
27. Gustafsson T and Ulfhake B: Aging skeletal muscles: What are the mechanisms of age-related loss of strength and muscle mass, and can we impede its development and progression?. Int J Mol Sci 25: 10932, 2024.
28. Xing HY, Liu N and Zhou MW: Satellite cell proliferation and myofiber cross-section area increase after electrical stimulation following sciatic nerve crush injury in rADAMTS-1. Chin Med J (Engl) 133: 1952-1960, 2020.
29. Meng J, Lv Z, Chen X, Sun C, Jin C, Ding K and Chen C: LBP1C-2 from Lycium barbarum maintains skeletal muscle satellite cell pool by interaction with FGFR1. iScience 26: 106573, 2023.
30. Agarwal M, Sharma A, Kumar P, Kumar A, Bharadwaj A, Saini M, Kardon G and Mathew SJ: Myosin heavy chain-embryonic regulates skeletal muscle differentiation during mammalian development. Development 147: dev184507, 2020.
31. Wang Y, Xiao Y, Zheng Y, Yang L and Wang D: An anti-ADAMTS1 treatment relieved muscle dysfunction and fibrosis in dystrophic mice. Life Sci 281: 119756, 2021.
32. Mierzejewski B, Grabowska I, Michalska Z, Zdunczyk K, Zareba F, Irhashava A, Chrzaszcz M, Patrycy M, Streminska W, Janczyk-Ilach K, *et al*: SDF-1 and NOTCH signaling in myogenic cell differentiation: The role of miRNA10a, 425, and 5100. Stem Cell Res Ther 14: 204, 2023.
33. Buas MF and Kadesch T: Regulation of skeletal myogenesis by Notch. Exp Cell Res 316: 3028-3033, 2010.
34. Luo D, de Morree A, Boutet S, Quach N, Natu V, Rustagi A and Rando TA: Deltex2 represses MyoD expression and inhibits myogenic differentiation by acting as a negative regulator of Jmjd1c. Proc Natl Acad Sci USA 114: E3071-E3080, 2017.
35. Isesele PO and Mazurak VC: Regulation of skeletal muscle satellite cell differentiation by Omega-3 polyunsaturated fatty acids: A critical review. Front Physiol 12: 682091, 2021.
36. Adhikari A, Kim W and Davie J: Myogenin is required for assembly of the transcription machinery on muscle genes during skeletal muscle differentiation. PLoS One 16: e0245618, 2021.
37. Faralli H and Dilworth FJ: Turning on myogenin in muscle: A paradigm for understanding mechanisms of tissue-specific gene expression. Comp Funct Genomics 2012: 836374, 2012.
38. Owens J, Moreira K and Bain G: Characterization of primary human skeletal muscle cells from multiple commercial sources. In Vitro Cell Dev Biol Anim 49: 695-705, 2013.
39. Ding R, Horie M, Nagasaka S, Ohsumi S, Shimizu K, Honda H, Nagamori E, Fujita H and Kawamoto T: Effect of cell-extracellular matrix interaction on myogenic characteristics and artificial skeletal muscle tissue. J Biosci Bioeng 130: 98-105, 2020.
40. Sanvee GM, Bouitbir J and Krähenbühl S: C2C12 myoblasts are more sensitive to the toxic effects of simvastatin than myotubes and show impaired proliferation and myotube formation. Biochem Pharmacol 190: 114649, 2021.
41. Henderson CA, Gomez CG, Novak SM, Mi-Mi L and Gregorio CC: Overview of the muscle cytoskeleton. Compr Physiol 7: 891-944, 2017.
42. Lehka L and Rędowicz MJ: Mechanisms regulating myoblast fusion: A multilevel interplay. Semin Cell Dev Biol 104: 81-92, 2020.
43. Lazure F, Blackburn DM, Corchado AH, Sahinyan K, Karam N, Sharanek A, Nguyen D, Lepper C, Najafabadi HS, Perkins TJ, *et al*: Myf6/MRF4 is a myogenic niche regulator required for the maintenance of the muscle stem cell pool. EMBO Rep 21: e49499, 2020.
44. Krampert M, Kuenzle S, Thai SN, Lee N, Iruela-Arispe ML and Werner S: ADAMTS1 proteinase is up-regulated in wounded skin and regulates migration of fibroblasts and endothelial cells. J Biol Chem 280: 23844-23852, 2005.

45. Dungan CM, Murach KA, Zdunek CJ, Tang ZJ, Nolt GL, Brightwell CR, Hettinger Z, Englund DA, Liu Z, Fry CS, *et al*: Deletion of SA β-Gal+ cells using senolytics improves muscle regeneration in old mice. Aging Cell 21: e13528, 2022.
46. Always SE, Paez HG, Pitzer CR, Ferrandi PJ, Khan MM, Mohamed JS, Carson JA and Deschenes MR: Mitochondria transplant therapy improves regeneration and restoration of injured skeletal muscle. J Cachexia Sarcopenia Muscle 14: 493-507, 2023.
47. Kim JW, Manickam R, Sinha P, Xuan W, Huang J, Awad K, Brotto M and Tipparaju SM: P7C3 ameliorates barium chloride-induced skeletal muscle injury activating transcriptomic and epigenetic modulation of myogenic regulatory factors. J Cell Physiol 239: e31346, 2024.
48. Wang YX and Rudnicki MA: Sataellite cells, the engines of muscle repair. Nat Rev Mol Cell Biol 13: 127-133. 2011.
49. Kerr HL, Krumm K, Anderson B, Christiani A, Strait L, Li T, Irwin B, Jiang S, Rybachok A, Chen A, *et al*: Mouse sarcopenia model reveals sex-and age-specific differences in phenotypic and molecular characteristics. J Clin Invest 134: e172890, 2024.
50. Owen AM and Fry CS: Decoding the decline: Unveiling drivers of sarcopenia. J Clin Invest 134: e183302, 2024.
51. Tao L, Huang W, Li Z, Wang W, Lei X, Chen J, Song X, Lu F, Fan S and Zhang L: Transcriptome analysis of differentially expressed genes and molecular pathways involved in C2C12 cells myogenic differentiation. Mol Biotechnol 67: 3640-3655, 2025.